The Journal of Neuroscience, August 1, 1996, 16(15):4537–4542

Apical Dendritic Location of Slow Afterhyperpolarization Current in Hippocampal Pyramidal Neurons: Implications for the Integration of Long-Term Potentiation

Pankaj Sah[1] **and John M. Bekkers**[2]

[1]*Neuroscience Group and the Discipline of Physiology, University of Newcastle, New South Wales, Australia, and* [2]*Division of Neuroscience, John Curtin School of Medical Research, Australian National University, Canberra, Australia*

Trains of action potentials in hippocampal pyramidal neurons are followed by a prolonged afterhyperpolarization (AHP) lasting several seconds, which is attributable to the activation of a slow calcium-activated potassium current (sI_{AHP}). Here we examine the location of sI_{AHP} on CA1 pyramidal neurons by comparing it with two GABAergic inhibitory postsynaptic currents (IPSCs) with known somatic and dendritic locations. Whole-cell patch-clamp recordings were made from CA1 pyramidal neurons in acute hippocampal slices. Stepping the membrane potential at the peak of sI_{AHP} produced a relaxation ("switchoff") of the AHP current with a time constant of 7.4 ± 0.4 msec (mean ± SEM). The switchoff time constants for somatic and dendritic $GABA_A$ IPSCs were 3.5 ± 0.5 msec and 8.8 ± 0.3 msec, respectively. This data, together with cable modeling, indicates that active sI_{AHP} channels are distributed over the proximal dendrites within ~200 μm of the soma. Excitatory postsynaptic potentials (EPSPs) evoked in stratum (s.) radiatum had their amplitudes shunted more by the AHP than did EPSPs evoked in s. oriens, suggesting that active AHP channels are restricted to the apical dendritic tree. Blockade of the AHP during a tetanus, which in control conditions elicited a decremental short-term potentiation (STP), converted STP to long-term potentiation (LTP). Thus, activation of the AHP increases the threshold for induction of LTP. These results suggest that in addition to its established role in spike frequency adaptation, the AHP works as an adjustable gain control, variably hyperpolarizing and shunting synaptic potentials arising in the apical dendrites.

Key words: AHP; cable analysis; dendrite; long-term potentiation; potassium channel; short-term potentiation

Calcium influx during action potentials activates two distinct types of calcium-dependent potassium currents in hippocampal pyramidal neurons. One of these currents (I_C) is active during action potential repolarization, whereas the other, a slow calcium-activated potassium current (sI_{AHP}), causes a prolonged afterhyperpolarization (AHP) that follows trains of action potentials and leads to spike frequency adaptation (Madison and Nicoll, 1984; Lancaster and Nicoll, 1987). It is now clear that although BK-type calcium-activated potassium channels underlie I_C (Lancaster and Nicoll, 1987), the sI_{AHP} is generated by a different type of channel that is distinct from BK or SK channels (Sah, 1996).

It has generally been assumed that active AHP channels are uniformly distributed over the surface of CA1 pyramidal neurons (Traub et al., 1991; Jaffe et al., 1994), although there is no direct evidence to support this view. Because the activation of sI_{AHP} is triggered by calcium influx via voltage-gated calcium channels (Hotson and Prince, 1980; Schwartzkroin and Stafstrom, 1980; Sah and Isaacson, 1995), the distribution of calcium channels may provide clues about the localization of activated AHP channels. L-type calcium channels are concentrated near the soma and particularly at the origins of the major dendrites, whereas N-type channels are widely distributed over the dendritic membrane (Ahlijanian et al., 1990; Westenbroek et al., 1992; Mills et al., 1994). It is becoming clear that different types of calcium channels selectively activate different calcium-activated potassium currents (Viana et al., 1993; Sah, 1995). Furthermore, calcium imaging experiments indicate that after action potentials, the highest levels of intracellular calcium are achieved in the proximal dendrites (Miyakawa et al., 1992; Regehr and Tank, 1992; Jaffe et al., 1994; Spruston et al., 1995). This raises the possibility that activated AHP channels also may have a restricted dendritic localization. Indeed, active AHPs can be recorded from the apical dendrites (Lancaster and Zucker, 1994; Andreason and Lambert, 1995). Because the AHP has a very slow time course (Lancaster and Adams, 1986; Sah and Isaacson, 1995) and responds to both calcium influx and many neuromodulators (Nicoll, 1988), an inhomogeneous distribution of active AHP channels would have major implications for the processing and integration of synaptic inputs.

In this article we address the question of the location of functioning AHP channels in hippocampal pyramidal neurons. Our findings indicate that these channels are selectively located in the proximal apical dendritic tree. Somatic AHP channels seem to contribute little to the net AHP conductance in these neurons.

MATERIALS AND METHODS

Electrophysiology. Hippocampal slices (400 μm thick) were prepared from 18- to 21-d-old rats using standard techniques (Sah and Isaacson, 1995). Slices were superfused with a Ringer's solution containing (in mM): 119 NaCl, 2.5 KCl, 1.3 Mg_2SO_4, 4.5 $CaCl_2$, 1 NaH_2PO_4, 26.2 $NaHCO_3$, and 11 glucose, which was equilibrated with 5% CO_2/95% O_2. Patch electrodes were filled with an internal solution containing (in mM): 135 $KMeSO_4$, 8 NaCl, 10 HEPES, 2 Mg_2ATP, and 0.3 Na_3GTP, pH 7.3 with KOH

Received Feb. 20, 1996; revised May 2, 1996; accepted May 7, 1996.

This work was supported by grants from the National Health and Medical Research Council of Australia, the Clive and Vera Ramaciotti Foundations, and the Australian Research Council. We thank Dirk van Helden and Stephen Redman for support, and Bob Callister, Stephen Redman, and Bruce Walmsley for suggestions.

Correspondence should be addressed to Dr. Pankaj Sah, Neuroscience Group, Discipline of Physiology, Faculty of Medicine and Health Sciences, University of Newcastle, New South Wales 2308, Australia.

(osmolarity 290 mOs/kg). Whole-cell patch-clamp recordings were obtained from CA1 pyramidal neurons using the "blind" approach (Blanton et al., 1989). Currents were recorded using an Axopatch-1D (Axon Instruments, Foster City, CA; bandwidth >10 kHz), filtered at 5 kHz, and sampled at 10 kHz using pClamp software (Axon Instruments). sI_{AHP}s were evoked by a 50–200 msec depolarizing voltage step to 0 mV. Series resistance was monitored carefully and noted for each cell. In experiments where $GABA_A$ inhibitory postsynaptic currents (IPSCs) were measured, 6-cyano-7-nitroquinoxaline-2,3-dione (CNQX; 10 μM) and D-2-amino-5-phosphonopentanoic acid (D-APV; 50 μM) were added to the perfusing medium to block polysynaptic events and reduce the spread of excitation. Somatic IPSPs were evoked by a bipolar stimulating electrode placed on the surface of the slice over stratum (s.) pyramidale. Dendritic IPSCs were evoked by placing another stimulating electrode near the border of s. radiatum and s. lucidum (Pearce, 1993). To measure the time course of the "switchoff," the reversal potential of the $GABA_A$ IPSC was measured, and then the holding potential was set 15 mV more depolarized. Steps from this holding potential (−48 to −51 mV) to the reversal potential were alternated with and without stimulation of the afferents. Traces were pairwise-subtracted, and 10 such subtractions were averaged. A similar procedure was used for the AHP switchoffs, except that a 15 mV hyperpolarizing step was always made from −50 mV. AHP and GABA switchoffs were bracketed several times on the same cell, and series resistance was checked for stability before and after each set of subtractions. Note that to facilitate comparisons, the stimulus intensity for the IPSCs was adjusted to elicit currents similar in amplitude to the AHP current measured in the same cell.

In experiments measuring shunting of basal and apical excitatory postsynaptic potentials (EPSPs), stimulating electrodes were placed in s. oriens and in the distal third of s. radiatum, and picrotoxin (100 μM) was added to block $GABA_A$ synaptic potentials that may have contaminated the peak of the synaptic potential. We noted that a higher concentration of isoprenaline (10 μM) was needed to block the AHP in whole-cell recordings (see Fig. 3*C*), compared with intracellular or field recordings (0.1–0.2 μM) (Madison and Nicoll, 1986) (see Fig. 4), perhaps because of partial washout. This higher concentration produced a small inhibition of EPSPs (see Fig. 3*C*, *right*). For LTP experiments, field EPSPs were recorded using a Ringer's solution-filled patch electrode. In each slice, an input/output curve was first measured, and the field EPSP amplitude was adjusted so that a half-maximal response was obtained.

Switchoff experiments were carried out at 30°C to increase the amplitude of the AHP and speed up its time course; shunting and LTP experiments were carried out at room temperature (~22°C). Statistical comparisons were made using the paired *t* test. All chemicals were obtained from Sigma (St. Louis, MO) except CNQX and D-APV, which were from Tocris Neuramin (Bristol, UK).

Cable modeling. Simulations were performed using NEURON, a program for numerically solving the cable equations in a compartmental model of a neuron (Hines, 1993). The model used the CA1 pyramidal cell shown in Figure 4 of Major et al. (1993), after its apical dendrites were collapsed further into a single equivalent dendrite. The accuracy of the collapsed model, compared with the full model, has been confirmed by Major et al. (1993). Equivalent cylinders were divided into compartments that were ≤10 μm (<0.01 λ). The passive properties of the model neuron were assumed to be uniform, with R_i = 100 Ωcm, C_m = 0.7 μFcm^{-2} (Major et al., 1993), and R_m chosen so that the model gave the input resistance measured for each neuron (R_m range 40–50 $k\Omega cm^2$). The model also incorporated the electrode series resistance measured for each switchoff experiment (range 8–15 MΩ). The somatic leak conductance was set at zero (Spruston and Johnston, 1992). For each simulation, the GABA or AHP conductance was either injected at a single site on the equivalent apical dendrite or was given a constant density ($S/\mu m^2$) over one or more equivalent cylinders. First, under simulated voltage clamp at the soma (without switchoff), both the amplitude and time course of the conductance were adjusted to match the current observed experimentally at the soma. The simulated switchoff current was then calculated and compared with the experimental trace. This process was repeated for many different injection sites or distributions over the equivalent dendrite. For the EPSP shunting simulations, the same model neuron was used in current clamp. The EPSP conductance was assumed to be described by an α function with τ = 3 msec and was injected at a point 300 μm from the soma into the equivalent basal or apical dendrite. $GABA_A$-mediated synaptic currents are weakly voltage-dependent (Collingridge et al., 1984); however, including this voltage-dependence in the model had minimal effects on the time course of the switchoff. The current underlying the AHP is voltage-independent (Lancaster and Adams, 1986).

RESULTS

We have used an indirect route to address the question of the location of active AHP channels. Consider a perfectly space-clamped cell that has a voltage-independent conductance. If the cell is voltage-clamped at a potential different from the reversal potential, a steady current will be measured by the voltage clamp. If the clamp potential is suddenly stepped to a different value, the membrane potential and membrane current will relax to their new values, with a time course determined by the speed of the voltage-clamp circuit, the series resistance of the electrode, and the capacitance of the cell (Jackson, 1992). In an extended structure such as a pyramidal neuron, however, distant dendritic membrane will settle more slowly to the new membrane potential after a voltage step imposed at the soma, because of the cable properties of the dendrites (Jack et al., 1983). As a consequence, relaxation of the membrane current arising in distant membrane will also be slowed, and current of increasingly distant origin will be slowed to an increasing extent (for review, see Spruston et al., 1994).

To test this prediction we took advantage of the anatomy of hippocampal pyramidal neurons, which receive fast inhibitory synaptic inputs from two distinct sets of GABAergic interneurons. One set forms baskets of synapses around the somas of pyramidal neurons (Andersen et al., 1964). The other set forms inhibitory synapses on the apical dendritic tree (Alger and Nicoll, 1982a). These two sets of interneurons can be stimulated selectively *in vitro* in a transverse hippocampal slice (Alger and Nicoll, 1982a; Pearce, 1993).

CA1 pyramidal neurons were voltage-clamped near −50 mV, and inhibitory postsynaptic currents (IPSCs) were evoked either by stimulation in the cell body region (somatic IPSC) or in s. radiatum (dendritic IPSC; Fig. 1*A*). Both IPSCs were blocked completely by picrotoxin (100 μM; n = 3), confirming that they were mediated by $GABA_A$ receptors. Near the peak of the synaptic current, the membrane potential was stepped to the reversal potential of the IPSC (near −65 mV). After the voltage step, the synaptic current relaxed to its new value with a time course that was faster for the somatic IPSC (τ = 3.5 ± 0.5 msec, mean ± SEM; n = 5) than for the dendritic IPSC (τ = 8.8 ± 0.3 msec; n = 4), consistent with its electrotonically closer location to the recording electrode at the soma ($p < 0.001$, paired *t* test; Fig. 1*B*). Note that the somatic relaxation is not instantaneous because the voltage-clamp step at the soma is slowed by the resistance of the electrode in series with the cell capacitance (Jackson, 1992). To determine the relaxation time course for the AHP current, sI_{AHP} was evoked by a 50–200 msec step to 0 mV from a holding potential of −50 mV. Near the peak of the outward current, the membrane potential was stepped to −65 mV. The current relaxed to its new value with a time constant of 7.4 ± 0.4 msec (n = 8), slower than that for the somatic $GABA_A$ IPSC ($p < 0.001$), but not significantly different from that for the dendritic IPSC ($p > 0.05$; Fig. 1*C*). These results suggest that active AHP channels are not concentrated on the soma.

To estimate the electrotonic locations on the neuron that would be compatible with these relaxation times, we constructed an equivalent cable model of a CA1 pyramidal cell (Fig. 2*C*; for details, see Materials and Methods). Varying the distribution of the synaptic conductance over the model cell, we found that the somatic $GABA_A$ relaxation was simulated best when the conductance was placed on the soma of the model (Fig. 2*A,B*, *left panels*,

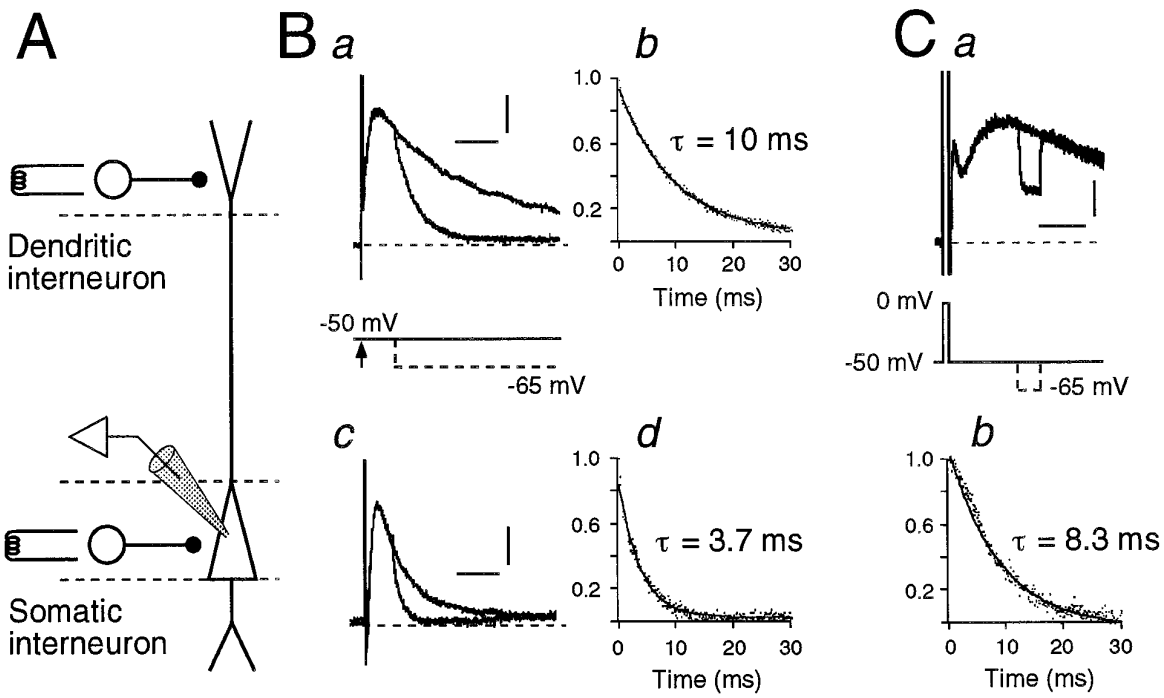

Figure 1. Current generating the AHP has a more distal distribution than current underlying the somatic GABAergic IPSC. *A*, Schematic diagram illustrating the experimental setup. The cell was voltage-clamped at the soma at a holding potential of −50 mV. Somatic and dendritic inhibitory postsynaptic currents (IPSCs) were independently stimulated in s. pyramidale and s. radiatum, respectively. Excitatory postsynaptic currents were blocked with CNQX (10 μM) and D-APV (50 μM). *B*, *a* and *c* show superimposed traces with and without a voltage step to the IPSC reversal potential (−65 mV). The stimulus protocol is shown in the *inset*; *arrow* indicates synaptic stimulation. The relaxations after the voltage step are shown expanded in *b* and *d* and have been fitted with a single exponential for comparison. As expected for an electrotonically distant input, the dendritic IPSC (*a*, *b*) relaxed at a slower rate (τ = 10 msec) than the somatic IPSC (*c*, *d*; τ = 3.7 msec) recorded in the same cell. *C*, The AHP current in the same neuron, with and without a voltage step to −65 mV (*a*). The current relaxation is shown expanded in *b* and has been fitted with a single exponential. The AHP current relaxed with a time course (τ = 8.3 msec) slower than that of the somatic IPSC, indicating that it must have a large contribution from extra-somatic channels. Calibration: 50 pA, 20 msec (*B*, *a* and *c*); 50 pA, 200 msec (*Ca*).

and 2*Ca*, *filled region*). In contrast, the AHP current relaxation was fitted best when the conductance change was either distributed over the equivalent proximal dendrite within ~200 μm of the soma (Fig. 2*Cb*, *filled region*) or injected at a point 50–100 μm from the soma (Fig. 2*Cb*, *arrow*) in different cells (n = 5; Fig. 2*A,B*, *right panels*). The AHP relaxation was clearly not fitted by a conductance concentrated at the soma. For the dendritic $GABA_A$ transient, the conductance had to be distributed further out in the dendrite, or injected at a point 100–125 μm along the equivalent dendrite from the soma, to predict correctly the transient (not shown). In two cells, we were also able to measure a $GABA_B$ IPSC that is thought to have a distant dendritic location (Alger and Nicoll, 1982b). In both cases, the time course of the relaxation was very slow (time constants 16.9 and 16.5 msec), consistent with a distant location for this conductance.

Hippocampal pyramidal neurons are polarized cells with a basal and an apical dendritic tree. We next asked whether the AHP conductance was located preferentially in either or both trees. To address this question, we took advantage of the laminar nature of the excitatory synaptic inputs to pyramidal neurons (Andersen et al., 1980). Because the decay time constant of the excitatory synaptic currents (3–5 msec; Hestrin et al., 1990) is faster than the membrane time constant (20–30 msec; Spruston and Johnston, 1992), the peak amplitude of a subthreshold EPSP reflects the local input impedance rather than the impedance of the whole cell (Carlen and Durand, 1981). EPSPs were evoked in either s. radiatum or s. oriens, alone or during the AHP (Fig. 3*A*). The peak amplitude of the EPSP in s. radiatum was reduced during the AHP (to 0.81 ± 0.04 of control, mean ± SEM; n = 8), whereas the EPSP evoked in s. oriens was affected marginally (0.98 ± 0.07; n = 8; Fig. 3*B*; s. radiatum and s. oriens are significantly different: $p < 0.05$). When the AHP was blocked by application of isoproterenol (10 μM; n = 3) or carbachol (1 μM; n = 2), the shunting of the EPSP after a depolarizing voltage step was blocked completely (Fig. 3*C*). This result indicates that AHP channels are located preferentially in the apical dendritic tree. These observations were also reproduced by the model (not shown; see Materials and Methods).

What are the physiological consequences of a dendritic location of the AHP? The action of the AHP in shunting the amplitude of local EPSPs is reminiscent of shunting inhibition (Carlen and Durand, 1981). Inhibitory inputs to pyramidal neurons have a significant effect on processes requiring synaptic integration. In particular, blockade of $GABA_A$ inhibition reduces the threshold for the induction of long-term potentiation (LTP) (Wigstrom and Gustafsson, 1983). We thus tested whether activation of the AHP has a similar role. Field EPSPs in area CA1 were evoked at a frequency of 0.1 Hz. After a stable baseline was obtained, a weak tetanus (50 Hz, 0.5 sec) was delivered, which caused a potentiation that returned to baseline over the next 30 min (Fig. 4*A*). The AHP was then reduced by application of the selective β-adrenergic agonist isoprenaline (Madison and Nicoll, 1986a). This concentration of isoprenaline had no effect on the control EPSP (Fig. 4*A*) or on the inhibitory postsynaptic potential (n = 2;

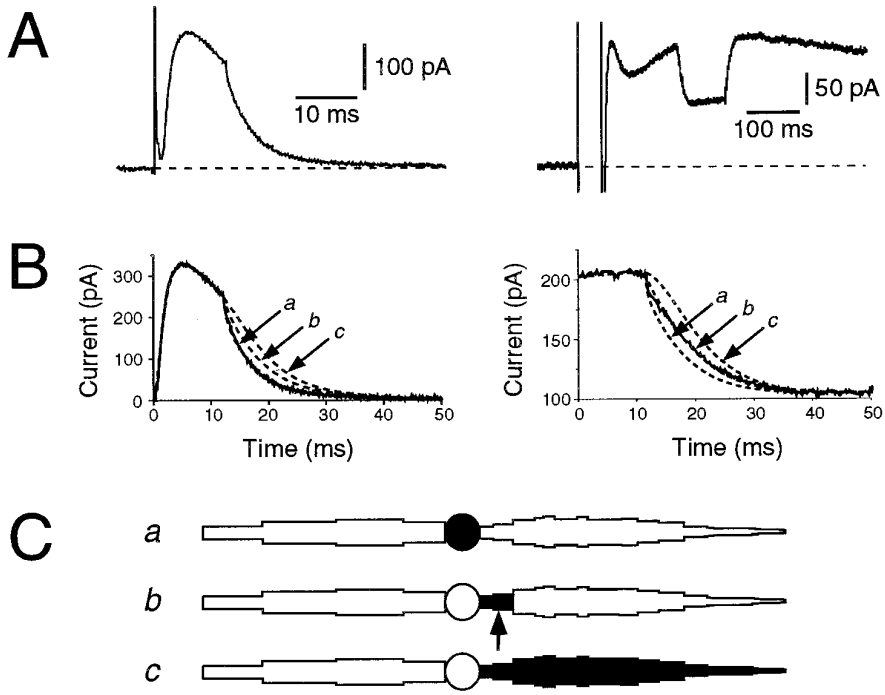

Figure 2. Electrotonic locations of the AHP and somatic $GABA_A$ IPSC channels, estimated using an equivalent cable model of a CA1 pyramidal neuron. *A*, Somatic IPSC (*left*) and AHP current (*right*) recorded in the same cell, when interrupted by a step from the holding potential (−50 mV) to −65 mV. *B*, The same currents shown expanded, with predictions from the model superimposed (*dashed lines*). Labels *a–c* correspond to different channel distributions in the model shown in *C*. Trace *a* (soma) best fits the IPSC switchoff, and trace *b* (proximal apical dendrite) best fits the AHP. *C*, Schematic diagram showing the equivalent cylinder model used to fit the data. The dendritic trees (apical at *right*) are shown to scale, using a different scale for the lengths and diameters, but the soma (*circle*) is not to scale. *Filled regions* represent the membrane surface that was given a constant conductance density: *a*, soma only; *b*, initial 166 μm of the apical dendrite; *c*, all of the apical dendrite. Adding the same conductance density to the soma made little difference to the predictions of models *b* and *c*, because the soma has a much smaller surface area than the dendrites. The *arrow* in *b* is 75 μm from the soma; injecting the AHP conductance at this point gave an identical switchoff to the distributed conductance in *b*.

not shown); however, the same weak tetanus delivered in the presence of isoprenaline produced a sustained potentiation (Fig. 4*A*; $n = 5$ slices). When the actions of isoprenaline at β receptors were blocked by co-application of the selective antagonist propranolol, the second weak tetanus also led to decremental potentiation, whereas a subsequent strong tetanus (100 Hz, 1 sec) produced a sustained potentiation (Fig. 4*B*).

DISCUSSION

In this article we have studied both the electrotonic location of the slow AHP current in hippocampal pyramidal neurons and its possible physiological role. We conclude that this current is localized to the proximal apical dendritic tree (within ~200 μm from the soma in the equivalent cable model), but relatively little of the current originates on the soma itself. This is based on two lines of evidence. (1) The switchoff of the AHP current was slower than that for a conductance located at the soma (Fig. 2), and (2) the amplitudes of EPSPs evoked in s. radiatum were shunted to a larger extent than those of EPSPs evoked in s. oriens (Fig. 3). If AHP channels were largely somatic, both EPSPs would be equally shunted (Carlen and Durand, 1981; our unpublished simulations). Note that our measurements can localize only active AHP channels; this distribution may reflect the inhomogeneous influx of calcium rather than the distribution of AHP channels themselves.

Although these experiments show clearly that the AHP conductance is not restricted to the somas of CA1 pyramidal cells, our conclusion about its exact dendritic location is obviously model-dependent. We have made three assumptions in our simulations. (1) The neuron is purely passive, apart from the GABA, AHP, or EPSP conductances, (2) its passive properties are uniform, and (3) the conductances are either distributed uniformly over the surface of the model cell or injected at a single point on the equivalent dendrite. Assumption 1 seems to hold for the small (15 mV) hyperpolarizing voltage steps used here, because no time-varying currents, apart from the capacity transients, were apparent during the step without the AHP or IPSC. Even if such currents were present, they are unlikely to have been affected by the presence or absence of a small synaptic or AHP conductance and would have been subtracted out in our protocol. Assumption 2 is commonly accepted (Spruston and Johnston, 1992). Assumption 3 is the most parsimonious one that yields good fits to the data, although other more heterogeneous distributions may fit the switchoffs equally well. Nevertheless, it is qualitatively clear from our simulations that the active AHP conductance cannot be concentrated at the soma, and neither can it be significant in the distal dendritic tree (Fig. 2*B,C*). Note that distance along the equivalent dendrite is not a simple function of dendritic distance in the real cell, because it depends on the branching pattern. The first 100 μm or so of the apical tree of CA1 pyramidal cells, however, is dominated by a single thick process emanating from the soma (Major et al., 1993), and so for this region, dendritic distance will be nearly the same for both real and equivalent cells. It is attractive to suppose that AHP channels are concentrated here so they can act to gate incoming signals from more distal parts of the apical dendritic tree.

Tetanic stimulation of afferent fibers in area CA1 can lead to the generation of a form of synaptic plasticity called LTP. LTP is triggered by depolarization of the postsynaptic cell attributable to summation of EPSPs and unblock of NMDA channels, which allows the influx of extracellular calcium (Bliss and Collingridge, 1993). Tetani delivered at lower frequencies, below the threshold for induction of LTP, give rise to a decremental form of potentiation called short-term potentiation (STP) (Malenka, 1991). During trains of afferent stimuli, summation of EPSPs and generation of action potentials also activate the AHP (Nicoll, 1988; Sah, 1996). This would reduce calcium influx through NMDA channels both directly, via the AHP hyperpolarization, and indirectly, by shunting EPSPs and reducing their depolarizing drive (Fig. 3). Blockade of the AHP during a given tetanus would therefore result in a larger depolarization, a larger calcium influx, and a lower threshold for the induction of LTP (Fig. 4; also see Hopkins and Johnston, 1981). Because activation of the AHP is relatively slow, these experiments lend support to the idea that some min-

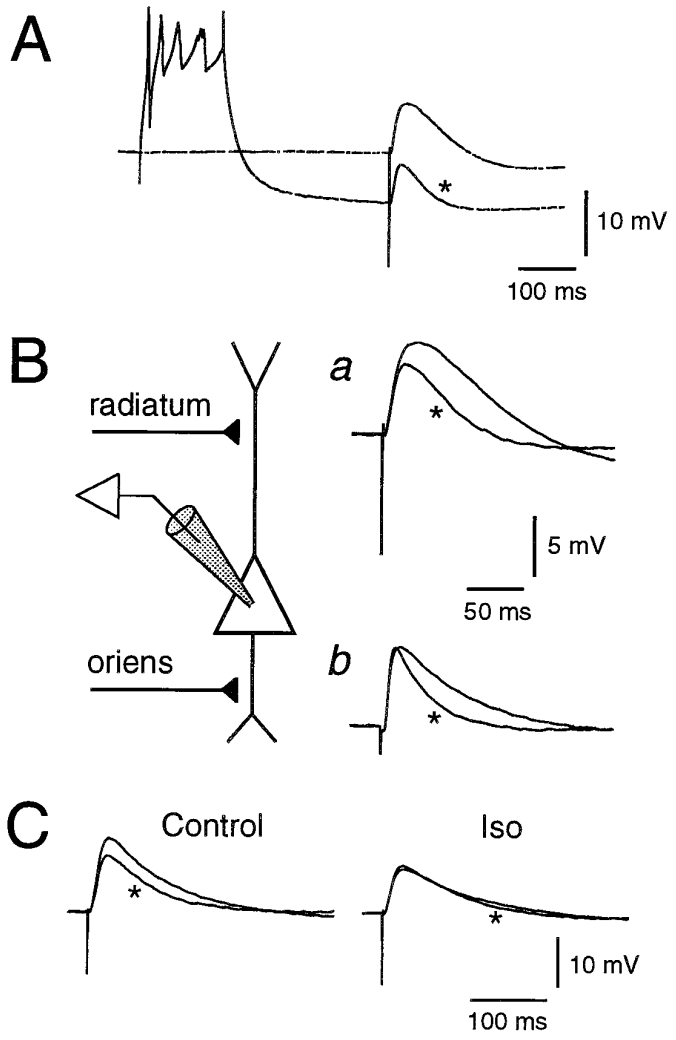

Figure 3. The AHP is preferentially located in the apical dendritic tree. *A*, Experimental paradigm. EPSPs were evoked with (*asterisk*) or without a preceding depolarizing current injection to activate the AHP. *B*, Current-clamp recordings were obtained from the soma, and EPSPs were evoked either in s. radiatum (*radiatum*) (*a*) or in s. oriens (*oriens*) (*b*). Fast IPSPs were blocked with picrotoxin (100 μM). Superimposed, baselined EPSPs are shown on the *right* with (*asterisk*) and without a concurrent AHP. The amplitude of the EPSP evoked in *radiatum* was preferentially shunted in comparison to the EPSP evoked in *oriens*. Note that the faster decay of the EPSPs with an AHP reflects the faster membrane time constant of the whole cell when the AHP is active. *C*, Control experiment showing that when the AHP is blocked by 10 μM isoprenaline (*Iso*, *right*), the shunting of the apical EPSP is absent. *Asterisks* identify the EPSPs obtained after the AHP-inducing stimulus.

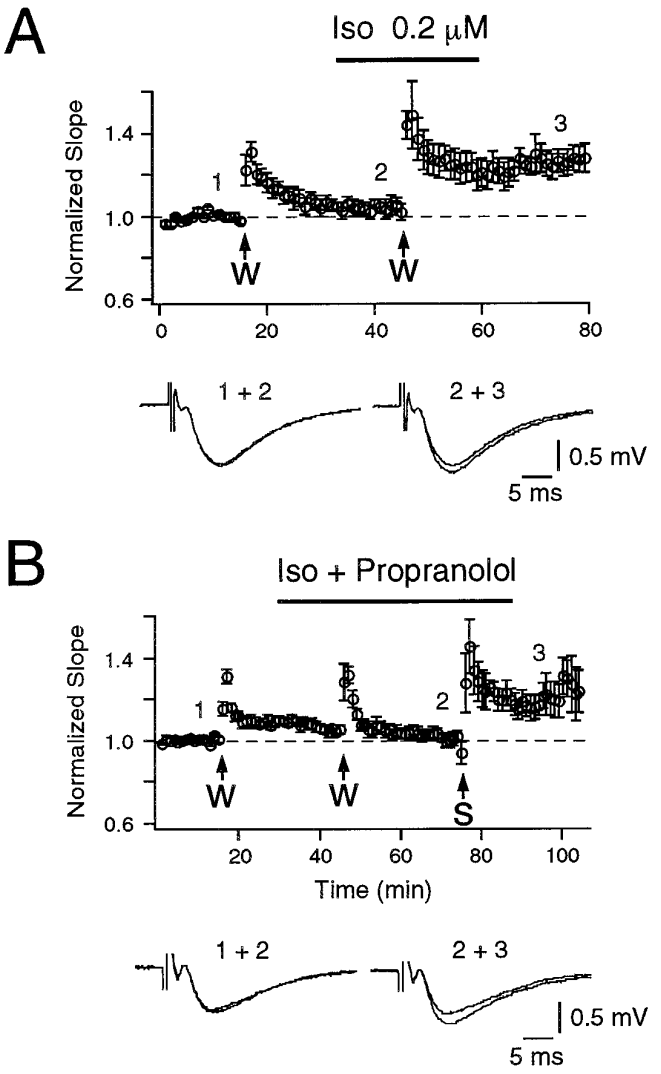

Figure 4. Blockade of the AHP converts STP into LTP. *A*, Graph of normalized field EPSP slope against time from experiments (n = 5 slices) where a weak tetanus (*W*; 50 Hz, 0.5 sec) was applied first by itself and then after blockade of the AHP with isoprenaline. A decremental potentiation (STP) is elicited by the first weak tetanus. When the AHP is blocked by isoprenaline (*Iso*; 0.2 μM), the same weak tetanus now elicits LTP. Sample field EPSPs are shown below for the times indicated. *B*, Graph of normalized field EPSP slope against time from experiments (n = 5 slices) where a weak tetanus (*W*; 50 Hz, 0.5 sec) was applied first by itself and then in the presence of isoprenaline plus propranolol (*Iso* + *Propranolol*) to block β-adrenergic receptors. Both times, the weak tetanus elicited STP. A subsequent strong tetanus (*S*; 100 Hz, 1 sec) elicited LTP, indicating that the slices were capable of potentiation. Sample field EPSPs are shown below for the times indicated.

imum duration of calcium influx is necessary to convert STP to LTP (Malenka, 1991; Malenka et al., 1992). It is notable that the threshold for LTP induction is lower in basal than in apical dendrites, a difference that is largely abolished by application of forskolin (Arai and Lynch, 1992). Forskolin increases cyclic AMP levels and blocks the AHP (Madison and Nicoll, 1986b). Thus, this finding is consistent with an apical location for AHP channels.

A number of neurotransmitter systems, including acetylcholine and norepinephrine, act via distinct second messenger systems to block the slow AHP. It is interesting that both cholinergic and monoaminergic transmitter systems have been implicated in the consolidation of memory (Squire, 1987). Activation of these systems and the subsequent blockade of the AHP would facilitate the induction of LTP. Although it remains possible that these second messenger systems interact in other ways with the generation of LTP (Chetkovich and Sweatt, 1993), blockade of the AHP could be one mechanism whereby these transmitters modulate the induction of LTP.

In conclusion, these studies show that the conductance generating the slow AHP in hippocampal pyramidal neurons is located predominantly in the proximal apical dendritic tree. Activation of this conductance during trains of action potentials acts as an adjustable gain control, short-circuiting the apical tree and preferentially shunting synapses impinging on the apical dendritic membrane.

REFERENCES

Ahlijanian MK, Westenbroek RE, Catterall WA (1990) Subunit structure and localization of dihydropyridine-sensitive calcium channels in mammalian brain, spinal cord and retina. Neuron 4:819–832.

Alger BE, Nicoll RA (1982a) Feed-forward dendritic inhibition of rat hippocampal pyramidal cells studied *in vitro*. J Physiol (Lond) 328:105–123.

Alger BE, Nicoll RA (1982b) Pharmacological evidence for two kinds of GABA receptor on rat hippocampal pyramidal cells studied *in vitro*. J Physiol (Lond) 328:125–141.

Andersen P, Eccles JC, Løyning Y (1964) Pathway of postsynaptic inhibition in the hippocampus. J Neurophysiol 27:608–619.

Andersen P, Silfvenius H, Sundberg SH, Sveen O (1980) A comparison of distal and proximal dendritic synapses on CA1 pyramids in guinea pig hippocampal slices *in vitro*. J Physiol (Lond) 307:273–299.

Andreason M, Lambert JDC (1995) The excitability of CA1 pyramidal cell dendrites is modulated by a local Ca^{2+}-dependent K^+- conductance. Brain Res 698:193–203.

Arai A, Lynch G (1992) Factors regulating the magnitude of long-term potentiation induced by theta pattern stimulation. Brain Res 598:173–184.

Bliss TVP, Collingridge GL (1993) A synaptic model of memory: long term potentiation in the hippocampus. Nature 361:31–39.

Carlen PL, Durand D (1981) Modelling the postsynaptic location and magnitude of tonic conductance changes resulting from neurotransmitters or drugs. Neuroscience 6:839–846.

Chetkovich DM, Sweatt JD (1993) NMDA receptor activation increases cyclic AMP in area CA1 of the hippocampus via calcium/calmodulin stimulation of adenylyl cyclase. J Neurochem 61:1933–1942.

Collingridge GL, Gage PW, Robertson B (1984) Inhibitory post-synaptic currents in rat hippocampal CA1 neurones. J Physiol (Lond) 356:551–564.

Hestrin S, Nicoll RA, Perkel DJ, Sah P (1990) Analysis of excitatory synaptic action in the rat hippocampus using whole cell recording from thin slices. J Physiol (Lond) 422:203–225.

Hines M (1993) NEURON: a program for simulation of nerve equations. In: Neural systems: analysis and modeling (Eeckman F, ed), pp 127–136. Norwell, MA: Kluwer Academic Publishers.

Hopkins WF, Johnston D (1981) Noradrenergic enhancement of long-term potentiation at mossy fiber synapses in the hippocampus. J Neurophysiol 59:646–657.

Hotson JR, Prince DA (1980) A calcium-activated hyperpolarization follows repetitive firing in hippocampal neurons. J Neurophysiol 43:409–419.

Jack JJB, Noble D, Tsien RW (1983) Electric current flow in excitable cells. Oxford: Clarenden.

Jackson MB (1992) Cable analysis with the whole-cell patch clamp: theory and experiment. Biophys J 61:756–766.

Jaffe DB, Ross WN, Lisman JE, Lasser-Ross N, Miyakawa H, Johnston D (1994) A model for dendritic Ca^{2+} accumulation in hippocampal pyramidal neurons based on fluorescence imaging measurements. J Neurophysiol 71:1065–1077.

Lancaster B, Adams PR (1986) Calcium-dependent current generating the afterhyperpolarization of hippocampal neurons. J Neurophysiol 55:1268–1282.

Lancaster B, Nicoll RA (1987) Properties of two calcium-activated hyperpolarizations in rat hippocampal neurones. J Physiol (Lond) 389:187–204.

Lancaster B, Zucker RS (1994) Photolytic manipulation of Ca^{2+} and the time course of slow, Ca^{2+}-activated potassium current in rat hippocampal neurones. J Physiol (Lond) 475:229–239.

Madison DV, Nicoll RA (1984) Control of repetitive discharge of rat CA1 pyramidal neurones in vitro. J Physiol (Lond) 354:319–331.

Madison DV, Nicoll RA (1986a) Actions of noradrenaline recorded intracellularly in rat hippocampal CA1 pyramidal neurones, *in vitro*. J Physiol (Lond) 372:221–244.

Madison DV, Nicoll RA (1986b) Cyclic adenosine 3′,5′-monophosphate mediates β-receptor actions of noradrenaline in rat hippocampal pyramidal cells. J Physiol (Lond) 372:245–259.

Major G, Evans JD, Jack JJB (1993) Solutions for transients in arbitrarily branching cables: I. Voltage recording with a somatic shunt. Biophys J 65:53–60.

Malenka RC (1991) Postsynaptic factors control the duration of synaptic enhancement in area CA1 of the hippocampus. Neuron 6:53–60.

Malenka RC, Lancaster B, Zucker RS (1992) Temporal limits on the rise in postsynaptic calcium required for the induction of long-term potentiation. Neuron 9:121–128.

Mills LR, Niesen CE, So AP, Carlen PL, Spigelman I, Jones OT (1994) N-type calcium channels are located on somata, dendrites and a subpopulation of dendritic spines on live hippocampal pyramidal neurons. J Neurosci 14:6815–6824.

Miyakawa H, Ross WN, Jaffe D, Callaway JC, Lasser-Ross N, Lisman JE, Johnston D (1992) Synaptically activated increases in Ca^{2+} concentration in hippocampal CA1 pyramidal cells are primarily due to voltage-gated Ca^{2+} channels. Neuron 9:1163–1173.

Nicoll RA (1988) The coupling of neurotransmitter receptors to ion channels in the brain. Science 241:545–551.

Pearce RA (1993) Physiological evidence for two distinct $GABA_A$ responses in rat hippocampus. Neuron 10:189–190.

Regehr WG, Tank DW (1992) Calcium concentration dynamics produced by synaptic activation of CA1 hippocampal pyramidal cells. J Neurosci 12:4202–4223.

Sah P (1995) Different calcium channels are coupled to potassium channels with distinct physiological roles in vagal neurons. Proc R Soc Lond [Biol] 260:105–111.

Sah P (1996) Calcium-activated potassium currents in neurons: types, physiological roles and modulation. Trends Neurosci 19:150–154.

Sah P, Isaacson JS (1995) Channels underlying the slow afterhyperpolarization in hippocampal pyramidal neurons: neurotransmitters modulate the open probability. Neuron 15:435–441.

Schwartzkroin PA, Stafstrom CE (1980) Effects of EGTA on the calcium activated afterhyperpolarization in hippocampal CA3 pyramidal cells. Science 210:1125–1126.

Spruston N, Johnston D (1992) Perforated patch-clamp analysis of the passive membrane properties of three classes of hippocampal neurons. J Neurophysiol 67:508–529.

Spruston N, Jaffe DB, Johnston D (1994) Dendritic attenuation of synaptic potentials and currents: the role of passive membrane properties. Trends Neurosci 17:161–166.

Spruston N, Schiller Y, Stuart G, Sakmann B (1995) Activity-dependent action potential invasion and calcium influx into hippocampal CA1 dendrites. Science 268:297–300.

Squire LR (1987) Memory and brain. Oxford: Oxford UP.

Traub RD, Wong RKS, Miles R, Michelson H (1991) A model of a CA3 hippocampal pyramidal neuron incorporating voltage-clamp data on intrinsic conductances. J Neurophysiol 66:635–650.

Viana F, Bayliss DA, Berger AJ (1993) Multiple potassium conductances and their role in action potential repolarization and repetitive firing behavior of neonatal rat hypoglossal motoneurons. J Neurophysiol 69:2150–2163.

Westenbroek RE, Hell JW, Warner C, Dubel SJ, Snutch TP, Catterall WA (1992) Biochemical properties and subcellular distribution of an N-type calcium channel α1 subunit. Neuron 9:1099–1115.

Wigstrom H, Gustafsson B (1983) Facilitated induction of hippocampal long-lasting potentiation during blockade of inhibition. Nature 301:603–604.